

Force Safety Device for Substation with Flexible Buses

Roman Miroshnik

Abstract - Short-circuit current sets the design loads for substation structure with flexible buses for voltage up to 115 kV and sometimes for higher voltage. Nonrecoverable Force Safety Device (FSD) being included in flexible buses can restrict the transmission of great unwanted forces to substation portals. The device operates similar to safety fuse of any electrical device while being replaced when tripped.

The paper deals with theoretical investigation of FSD usage efficiency. Two mathematical models (one is to verify another) are built: first model is based on the finite difference equations and the second one uses ANSYS finite elements program. The finite difference equations are derived by linearization of nonlinear equations of buses motion. Both models include bus conductor, insulators, FSD, portals masses and portals stiffness. Results of actual calculations, that show the efficiency of FSD are presented.

Index terms - short-circuit currents, bus, safety, portals, substations, nonlinear systems.

I. INTRODUCTION

The drastically short run increase of the short-circuit current (as compared with the operation conditions) results in significant mechanical stresses and deflections of substation flexible bus systems. The short-circuit current usually set the design loads for substation structures having flexible buses for voltage up to 115 kV and sometimes for higher voltage.

A nonrecoverable FSD being included in flexible buses restricts the transmission of great unwanted forces to portals. The FSD under consideration is located between one of bus insulators and portal. The scheme of FSD construction and its deformation is shown in Fig. 1.

The main detail of the FSD is a metallic cramp having two weakened cross section areas, which are calibrated to established beforehand actuation force P_{dev} . The cramp is connected to flexible buses through hinged strap. While the level of actuation force is achieved in the bus, the cramp is deformed plastically in the weakened area vicinities.

Because of construction simplicity FSD is much cheaper than the substation portals and can be economically sound. The FSD operates similar to safety fuse of any electrical device, while it is replaced when it is tripped (in our case residually deformed).

The FSD has piecewise-linear force displacement characteristic as shown in Fig.2. The characteristic includes two inclined (elastic) regions having different stiffnesses and the horizontal (plastic) region with constant resistance P_{dev} . The horizontal

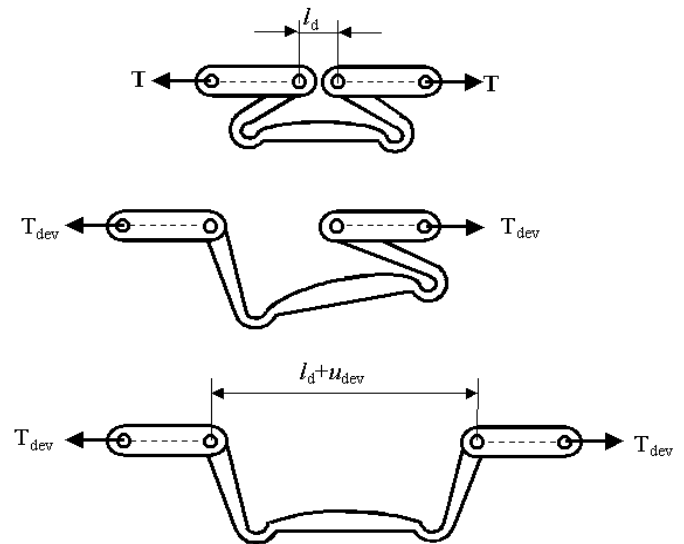


Fig. 1 Scheme of FSD construction and its deformation.

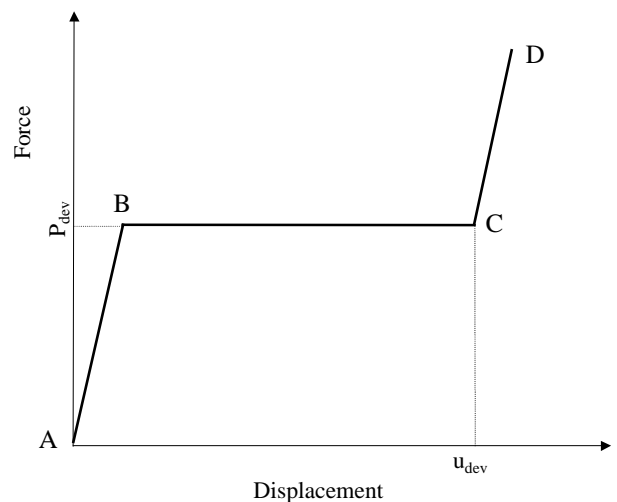


Fig. 2. Force - displacement characteristic of FSD. AB – first inclined elastic region, BC - the horizontal plastic region with constant resistance, CD – second inclined elastic region.

length of the characteristic (till level u_{dev} , which is established before) includes the FSD elastic and plastic displacement.

A safety device for portal overloading restriction during erecting of transmission line is described in [6], [7].

An approach to solution of cable dynamic under short-circuit current using finite difference equations is given in [3], [4]. Still these equations accumulate calculation errors and give satisfactory results only for short periods of time. The modified equations [5] used in this paper are free of such error accumulation.

Manuscript received March 23, 2003. This work was supported by the Israel Electric Corporation Ltd.

The author is with Israel Electric Corporation Ltd., Haifa, Israel, Expert Engineer (e-mail: mir@iec.co.il).

Digital Object Identifier 10.1109/TPWRD.2003.817491

This paper deals with the substation bus model presented in Fig. 3. The model includes conductor, two insulators, FSD, equivalent portal masses at two end points and two elastic constrains simulating portal stiffness.

The conductor and the insulators are simulated as perfectly flexible uniform extensible cables with corresponding properties (without compression, bending and torque stiffness). Conductor and insulators gravity is taken into consideration. Electromagnetic forces (described below) also load the conductor.

Because of convergence problems two mathematical models (one is to verify another) are built: first model is based on the finite difference equations of cable motion and the second one uses ANSYS finite elements program [2].

II. ELECTROMAGNETIC FORCES

An electric conductor carrying current $I_1(t_d)$, in a magnetic field due to another conductor carrying current $I_2(t_d)$ undergoes electromagnetic force F_d per unit conductor length:

$$F_d = \frac{\mu_0}{2\pi} \frac{I_1(t_d) I_2(t_d)}{a} \quad (1)$$

where μ_0 is the electromagnetic constant; a is the distance between the conductors.

According to the CIGRE recommendations [1] the short-circuit current $I(t_d)$ is defined as:

$$I(t_d) = I_a [\sin(\omega t_d + \xi_u - \gamma_z) + \sin(\gamma_z - \xi_u) e^{\frac{t_d}{\tau}}] \quad (2)$$

where I_a is the amplitude of the short-circuit current (at zero time); ξ_u, γ_z, τ are constants.

Likewise on the real system it is assumed that the short-circuit current spreads 0.1-0.2 sec whereupon the electrical power protection cut off it.

III. FINITE DIFFERENCES MODEL

The dynamic equations of the cable motion in the nondimensional form are [2]:

$$\begin{aligned} \lambda(1+\alpha T) \frac{\partial^2 X_i}{\partial t^2} - \frac{\partial}{\partial S_0} X; \\ \left(\frac{T}{1+\alpha T} \frac{\partial X_i}{\partial S_0} \right) - F_i(1+\alpha T) = 0 \\ \sum_{i=1}^3 \left(\frac{\partial X_i}{\partial S_0} \right)^2 = (1+\alpha T)^2 \\ \frac{\partial S}{\partial S_0} = 1 + \alpha T. \end{aligned} \quad (3)$$

where the term ‘‘cable’’ is used with corresponding properties both for bus conductor and insulators; X_i, F_i ($i = 1, 2, 3$), T, t, S_0, S are the nondimensional: ‘‘Cartesian coordinates’’, ‘‘external forces’’, ‘‘cable tension’’, ‘‘time’’, ‘‘arc undeformed and deformed cable coordinates’’, respectively; i is the Cartesian coordinates index (instead of x, y, z).

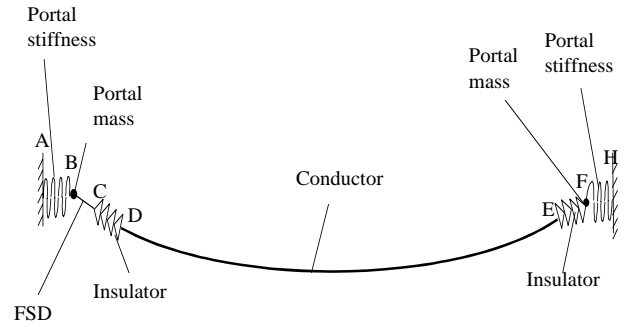


Fig. 3. The substation bus model. DE - conductor, CD, EF - insulators, BC - Force Safety Device, B, FH - flexible constrains simulating portal stiffness, B, F - equivalent portal masses at the end points.

The term ‘‘nondimensional’’ and quotes are omitted in the text below for above-mentioned values;

$$\begin{aligned} X_i &= \frac{X_{id}}{\ell}; & S &= \frac{S_d}{\ell}; & S_0 &= \frac{S_{d0}}{\ell}; \\ T &= \frac{T_d}{\beta mg \ell}; & F_i &= \frac{F_{di}}{\beta mg}; & t &= t_d \omega \end{aligned}$$

where T_d is the real bus tension; X_{id} are the real Cartesian coordinates of an arbitrary cable point; F_{di} are the projections of real external force on Cartesian axis; S_{d0}, S_d are the real arc (Euler) undeformed and deformed coordinates along bus (before and after loading respectively); t_d is the real time; β is nondimensional coefficient that equates the tension order with the order of the rest of variables. It depends on bus parameters and its value is between 100 to 10000; A_s is the area of bus cross section; E is the modulus of elasticity of bus material; m is the mass of bus length unit; g is the gravitational constant; $\ell = \ell_d + 2\ell_{is} + \ell_c$ is the undeformed bus length between two ends (before loading); $\ell_d, \ell_{is}, \ell_c$ are undeformed bus lengths of FSD, insulators and conductor respectively; ω is the current frequency of the electrical system; α, λ are nondimensional constants; $\alpha = \beta mg \ell / A_s E$ $\lambda = \ell \omega^2 / \beta g$.

There is a set of five equations of motion (3) for each of three cable parts of the bus model. First three equations deal with the spatial motion of an arbitrary point. The curvilinear coordinate S defines the deformed cable length until the arbitrary cable point. The fourth equation relates Cartesian coordinates with the coordinate S . The fifth equation connects the deformed cable length S with the undeformed one S_0 .

Two equivalent portal masses m_{pB}, m_{pF} and two elastic supports are considered at the end cable points B and F (Fig. 3). The boundary conditions for these points are:

$$\begin{aligned} k_{pB} X_{2B} - m_{pB} \frac{\partial^2 X_{2B}}{\partial t^2} = T \frac{\partial X_{2B}}{\partial S_0} \\ k_{pF} X_{2F} - m_{pF} \frac{\partial^2 X_{2F}}{\partial t^2} = T \frac{\partial X_{2F}}{\partial S_0} \end{aligned} \quad (4)$$

where X_{2B}, X_{2F} are the horizontal coordinates of the end points; k_{pB}, k_{pF} are the portal stiffnesses at the end points in horizontal direction.

The equations describing FSD behavior (characteristic) are:

$$X_{iB} - X_{iC} = k_d T_C \frac{\partial X_{iC}}{\partial S_0}, \text{ when } T < P_{dev} \text{ or } u > u_{dev}$$

$$T_B = T_C = P_{dev}, \text{ when } T = P_{dev} \text{ and } u \leq u_{dev} \quad (5)$$

where k_d is the stiffness of FSD first elastic region (Fig.2); X_{iB} , X_{iC} are the coordinates of FSD end points B, C; T_B, T_C are the tensions at FSD end points B, C.

The initial cable profile $\varphi_i(S_0)$ is known and may be calculated by one of the static methods (for instance [4]). This profile for cable, which is subjected only to gravity force, is the catenary line. When assuming zero initial speed of the cable, the initial conditions are

$$X_i(S_0, 0) = \varphi_i(S_0); \quad \frac{\partial X_i(S_0, 0)}{\partial t} = 0 \quad (6)$$

The cable linear increment equations are obtained by performing the following replacements in (3):

$$X_i = \tilde{X}_i + x_i, \quad T = \tilde{T} + h, \quad S = \tilde{S} + s, \quad F_i = \tilde{F}_i + f_i, \quad (7)$$

where $\tilde{X}_i, \tilde{T}, \tilde{S}, \tilde{F}_i$ are values corresponding to an arbitrary time t ; X_i, T, S, F_i are values corresponding to time $t + \Delta_t$; x_i, h, s are small increments of the coordinates, tension and arc length after small increment of time Δ_t ,

After manipulations while confining only the first-order terms in the equations we obtaine

$$\begin{aligned} \lambda \frac{\partial^2 x_i}{\partial t^2} - \tilde{T} \frac{\partial^2 x_i}{\partial S_0^2} - \frac{\partial^2 \tilde{X}_i}{\partial S_0^2} h - \frac{\partial \tilde{T}}{\partial S_0} \frac{\partial x_i}{\partial S_0} - \\ - \frac{\partial \tilde{X}_i}{\partial S_0} \frac{\partial h}{\partial S_0} + \lambda \frac{\partial^2 \tilde{X}_i}{\partial t^2} \alpha h - \tilde{F}_i \alpha h - f_i = 0 \\ \sum_{i=1}^3 \left(\frac{\partial \tilde{X}_i}{\partial S_0} \frac{\partial x_i}{\partial S_0} \right) - 2\alpha h = 0; \\ \frac{\partial s}{\partial S_0} = \alpha h \quad (i=1,2,3) \end{aligned} \quad (8)$$

Substitution (7) in (5),(6) leads to increment boundary equations:

$$\begin{aligned} k_{pB} x_{2B} - m_{pB} \frac{\partial^2 x_{2B}}{\partial t^2} = \tilde{T}_B \frac{\partial x_{2B}}{\partial S_0} + h \frac{\partial \tilde{X}_{2B}}{\partial S_0}; \\ k_{pF} x_{2F} - m_{pF} \frac{\partial^2 x_{2F}}{\partial t^2} = \tilde{T}_B \frac{\partial \tilde{X}_{2F}}{\partial S_0} + h \frac{\partial x_{2F}}{\partial S_0}; \end{aligned} \quad (9)$$

$$x_{iB} - x_{iC} = k_d T_C \frac{\partial x_{iC}}{\partial S_0} + k_d h_C \frac{\partial \tilde{X}_{iC}}{\partial S_0},$$

when $T < P_{dev}$ or $u > u_{dev}$;

$$h_B = h_C = 0, \text{ when } T = P_{dev} \text{ and } u \leq u_{dev}. \quad (10)$$

The finite difference equations are obtained after digitization of (8)-(10), while confining only the values of the same order as the increments x_i, h, s, f_i . These equations simulate the cable

motion using N cable points, $(N-1)$ cable linear elements of constant undeformed length Δ_{s0} and M constant time steps Δ_t . There is a set of algebraic linear equations with regard to 13 unknown quantities $x_{i,j-1}^{k+1}, x_{i,j}^{k+1}, x_{i,j+1}^{k+1}, h_{j-1}^{k+1}, h_j^{k+1}, s_j^{k+1}$ for time step $(k+1)$ ($k=1 \dots M$) and for each cable point j ($j=1 \dots N$). Each set connects the quantities at three cable points $(j-1), j, (j+1)$ for three time steps $(k-1), k, (k+1)$.

Thus, the system of algebraic equations for an arbitrary time step $(k+1)$ is:

$$\mathbf{A}\mathbf{Y} = \mathbf{B} \quad (11)$$

where \mathbf{A} is the band matrix depending on cable variables on time steps $(k-1), k$; \mathbf{B} is the free term vector of the equations system depending on cable variables on time steps $(k-1), k$; \mathbf{Y} is the vector of unknown cable quantities on time step $(k+1)$.

Band coefficients' matrix \mathbf{A} is positively defined. The solution of system (11) can be carried out while using standard programs. The equation system (11) is solved for each time step thus that the results from the preceding step are used as initial conditions for the next step.

Matrix \mathbf{A} is singular, when the cable tension is positive. In order to ensure nonsingularity of matrix \mathbf{A} the tension is zero filled during the computation procedure, if it becomes small negative one in the neighborhood of zero.

IV. FINITE ELEMENTS MODEL

The ANSYS finite elements model of the substation buses has the same configuration as shown in Fig. 3. Three next types of finite elements are used for:

- Uniaxial tension-only elements of type LINK10 for simulation of cables (conductor and insulators);
- Spring-Damper elements of type COMBIN14 for simulation of portals' masses and stiffnesses;
- Control elements of type COMBIN37 for simulation of FSD with its characteristic (Fig.3).

The transient nonlinear analyses are carried out on three stages.

On the first stage the equilibrium problem of the cable under gravity is solved as dynamic problem [2], while empirically found damping coefficients of surroundings are introduced. This stage is necessary to find the cable equilibrium mode and to exclude the cable vibrations during the gravity loading. Duration of this stage is about 1000 seconds with time step of 10 seconds.

On the second stage (during the short-circuit current action) the cable is loaded by additional electromagnetic forces (1). The transient solution with time step 0.001-0.002 seconds is carried out, while the electromagnetic forces change on each time step for each cable segment depending on distance between the buses.

During the third stage only gravity acts and the solution is obtained with the same time step as on the previous stage.

V. RESULTS OF CALCULATIONS AND DISCUSSION

The solution convergence for both models (of finite differences and finite elements ones) depends on correct choice

TABLE I.
PARAMETERS FOR COMPUTATION
CONVERGENCE

Parameter	Units	FD Method	FE Method
Number of conductor elements	-	50	25
Number of isolator elements	-	4	4
Time step	sec	0.0001-0.0005	0.001-0.002
Calculation accuracy	%	0.0005-0.001	0.05-0.1
Average run time	min	5	15

TABLE 2.
SUBSTATION BUSES AND FSD PARAMETERS

Symbol	Parameter	Units	Value
m_c	Conductor mass per unit length	kg/m	1.2
m_i	Isolator mass per unit length	kg/m	41
ℓ	Bus free length	m	20
ℓ_i	Insulator length	m	3.1
T_0	Stretch bus tension	N	2100
P_{dev}	FSD actuation force	N	5000
A_s	Conductor cross section area	mm ²	1500
E_c	Elasticity modulus of conductor	N/mm ²	5000
E_i	Elasticity modulus of insulator	N/mm ²	9000
t_c	Short-circuit current duration	sec	0.2
	Initial electromagnetic force per unit length	N/m	14

of relation between computation accuracy, time steps and amount of cable elements. One of the two models with once chosen parameters may converge while another model with the same parameters may not. This is the reason why two models are built, one is to verify another.

The conditions of computation convergence for both models are found empirically by trial-error method. Good convergence for two examples presented below is achieved for combination of computation parameters given in the Table 1.

Frequently, when the computation parameters are enough far from the noted domain, the result interpretations need additional care. For example, small time step or/and high accuracy cause appearance of dummy oscillations on moving trajectory. Big steps as well as computation inaccuracy may leads to rounding of trajectory and disappearing of the important details.

The use of two presented computation models having different parameter convergence domains, enable us to validate the obtained results. The results are considered as reliable if the two model solutions are practically close. Additional result validation is the convergence to physical feasible mode.

Two examples of calculations are made for a typical substation bus (with or without FSD) having parameters listed in Table 2.

The plots of the maximum bus tension versus time and the trajectories of bus span midpoint on the x-y plane are presented for two examples of calculations in Fig. 4, 5. Every figure contains the results corresponding to the substation bus with and without FSD.

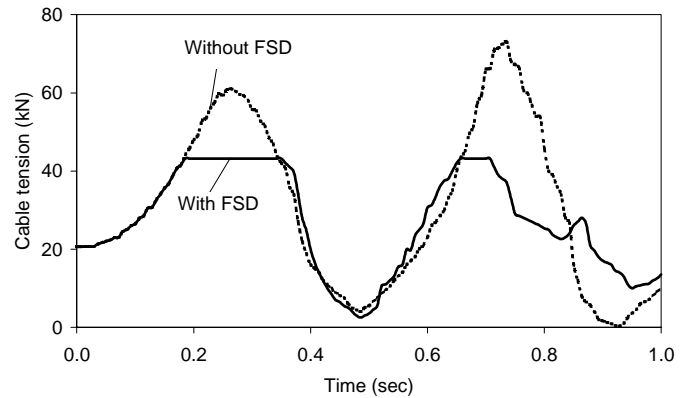


Fig. 4. Bus tension versus time. Continuous lines - the bus contains FSD, dotted lines - the bus without FSD.

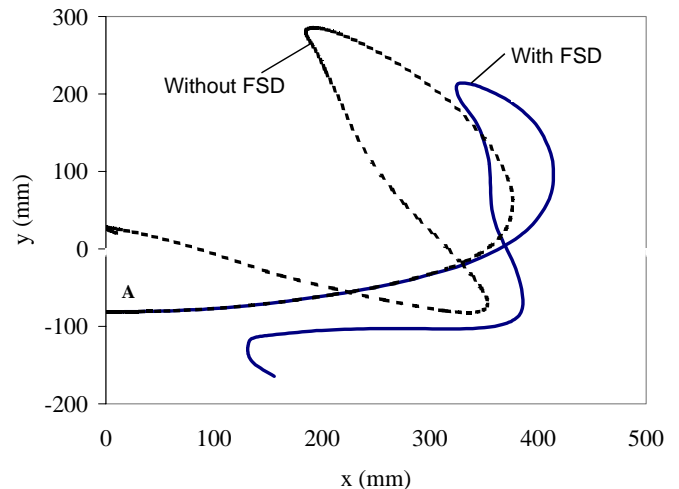


Fig. 5. Trajectories of bus span midpoint on the x-y plane. Continuous lines - the bus contains FSD, dotted lines - the bus without FSD. Beginning of time corresponds to the point A for both graphs.

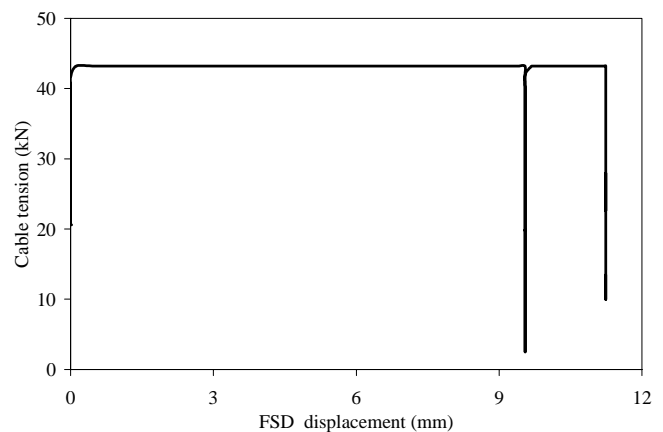


Fig. 6. Bus tension versus FSD displacement. Horizontal regions correspond to FSD plastic deformation (actuation force).

The plot of tension versus FSD displacement is shown in Fig. 6 and the plot of the same displacement versus time – in Fig. 7. The calculated dependence of maximum bus force on short-circuit current amplitude for Table 2 parameters is presented in Fig. 8 for the substation bus without FSD.

The parameters of FSD may be defined after establishing a small probability p_c of FSD trip during the chosen return period of years (5, 10 etc). Then, the maximum short-circuit

current corresponding to the established probability p_c is found [5].

The plot of tension versus FSD displacement is shown in Fig. 6 and the plot of the same displacement versus time – in Fig. 7. The calculated dependence of maximum bus force on short-circuit current amplitude for Table 2 parameters is presented in Fig. 8 for the substation bus without FSD.

The maximum bus force corresponding to maximum short-circuit current with established probability is found from Fig. 8. This value is used as FSD actuation force P_{dev} . The value of FSD actuation deformation u_{dev} (including plastic one) is established using the plot presented in Fig. 7.

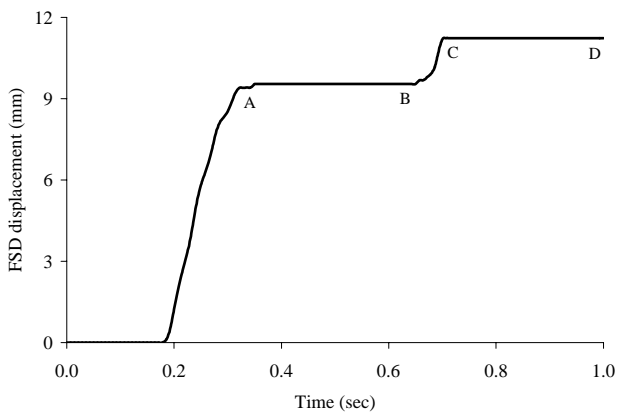


Fig. 7. FSD displacement versus time. AB, CD are regions of FSD plastic deformation.

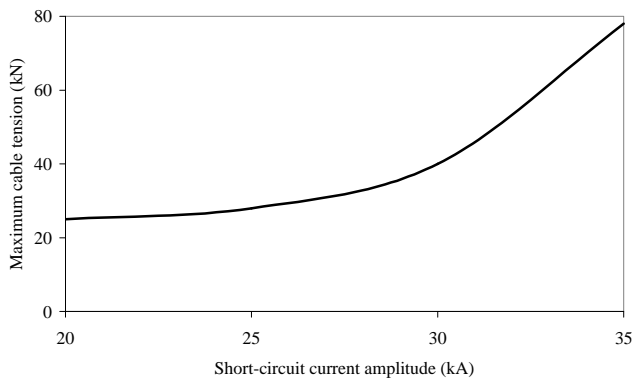


Fig. 8. Dependence of maximum bus tension on short-circuit current amplitude for bus without FSD.

During the return period the maximum short-circuit current causes FSD trip once on average. Consequently, the permanent (residual) bus sag increases at 4.2% and the permanent tension decreases at 4.1% (while considering residual displacement). These changes do not need immediate interference in substation operation and are acceptable for a period of time that is enough to replace FSD.

VI. CONCLUSION

Nonrecoverable force safety device prevents the transmission of unwanted loads to substation portals during the short circuit current. FSD can be economically sound. FSD trip occurs once on average during the return period with the probability established beforehand. FSD, which is tripped, is replaced with the new one. The calculation results show that FSD enables us to decrease significantly the loads translated to the portals.

VII. ACKNOWLEDGMENT

The author gratefully acknowledges the contribution of Dr. D. Laredo and Dr. H. B. Haim for their work on the discussion of the paper results and his daughter Elena for paper edition.

VIII. REFERENCES

Standards:

- [1] The Mechanical effects of short-circuit currents in open-air substations, CIGRE WG 02, 1987.

Books:

- [2] ANSYS Basic Analysis Guide, ANSYS Software, Revision 5.7.1, ANSYS Inc., 2002.

Periodicals:

- [3] P. Roussel, "Numerical solution of static and dynamic equations of conductor," *Comp. Meths. App. Mech. Eng.* 9, 1976.
- [4] A. M. Watts & R. H. Frith, "Efficient numerical solution of the dynamic equations of conductors," *Comp. Meths. App. Mech. Eng.* 25, 1981.
- [5] R. Miroshnik, "The probabilistic model of the dynamic of the cables under short-circuit current," *Comp. Meths. App. Mech. Eng.*, 187, 2000, pp. 201-211.

Internet

- [6] *The Sicame group in France*, http://www.sicame.fr/anglais/sef_0500.htm
- [7] *The Group Sicame, Dervaux Distribution, Omega, Strain device controlled lengthening type*, 2002

IX. BIOGRAPHY



Roman Miroshnik was born in Moldova, on July 12, 1945. He graduated from the Moscow State Technical University named after N. E. Bauman in 1970. He received his Ph. D. (1973) and D. Sc. (1990) degrees in Mechanical Engineering in the same University. He has been involved, in particular, with research and development projects for static and dynamics of flexible bars. From 1992 he is engaged in R&D Division of Israel Electric Corp. His current interests include development of probabilistic and deterministic approach to dynamics of electrical transmission lines under short-circuit current. The author has about 70 scientific publications.